DIGITAL DESIGN OF BROADBAND LONG-PERIOD FIBRE GRATINGS BY AN INVERSE SCATTERING ALGORITHM WITH FLIP-FLOP OPTIMISATION

R. Kritzinger*, J. Burger*, J. Meyer and P. L. Swart†**

** Optical Frequency Standards and Photonics Technology Group, R&D Core, National Metrology Institute of South Africa, Private Bag X34, Lynnwood Ridge, Pretoria, 0040, South Africa. E-mail: rkritzinger@nmisa.org*
*** Department of Electrical and Electronic Engineering Science, Photonics Research Group, University of Johannesburg, P. O. Box 524, Auckland Park, 2006, South Africa.*
E-mail: johanm@uj.ac.za
† Deceased

Abstract: A discrete inverse scattering method, known as layer-peeling, is used to synthesise a LPFG (long-period fibre grating) from a desired complex spectrum by a direct solution of the coupled-mode equations, while simultaneously determining the physical properties of the layered structure. The physical properties of the grating structure are determined in a recursive layer-by-layer manner by using causality arguments to design LPFGs exhibiting a flat-top spectral profile. The results obtained from the layer-peeling method are optimised using the flip-flop method to ease the fabrication process. We found that the layer-peeling method has the highest performance and executes in the least amount of time. A discussion of possible applications where optimised broadband LPFGs could be utilised in the field of telecommunications and sensing demonstrates the importance of the results.

Keywords: Long-period fibre grating, complex spectrum, layer-peeling, flip-flop method.

1. INTRODUCTION

Over the years, it has become important to design appropriate optical filters, for example LPFGs, to achieve a desired spectral response. LPFGs are transmission-type spectral filters that can be used in various applications with their guided-to-cladding mode power exchange, for example as gain equalisers for erbium-doped fibre amplifiers (EDFAs) [1], as channel routers in optical add-drop multiplexers (OADMs) [2] or as sensors [3].

LPFG synthesis entails the derivation of the physical properties of a transmission filter from a desired spectral response [4, 5]. The grating synthesis problem is by no means trivial, especially compared to the well-known problem of computing the spectrum directly from a specific grating structure [6]. When designing fibre gratings, care should be taken to strictly monitor the complexity of the index modulation of the grating structure, such that it can be practically realised in the optical fibre core during the grating fabrication process, which was one of the aims of this research as well.

It has been shown that LPFG structures (e.g. exhibiting a flat-top spectral profile) can be reconstructed fast and efficiently from a desired complex spectrum using the discrete layer-peeling (DLP) method [4, 5]. The physical properties of a grating structure are calculated in a recursive layer-by-layer manner by using causality arguments. This method is stable and has a low algorithmic complexity that scales as $O(M^2)$. Genetic algorithms (GAs) and variational optimisation can also used to synthesise LPFGs [7, 8]. However, these methods have a low algorithmic efficiency and a slow convergence when complex LPFGs are designed. In this paper, the DLP method and flip-flop optimisation method are used to design LPFGs to achieve a desired spectral response. The flip-flop method has been known to be effective in designing interference coatings and rugate filters [9]. The flip-flop method is used to optimise a DLP synthesised LPFG to exhibit either a low or high index change at each grating period to ease the grating fabrication process. Possible applications are also discussed where synthesised LPFGs could be utilised.

2. BACKGROUND

2.1 Grating synthesis by layer-peeling algorithm

During the synthesis of an LPFG, the grating structure and physical properties are derived from a desired spectral profile utilising the transfer matrix model [4-6]

$$\begin{bmatrix} R_j(\delta) \\ S_j(\delta) \end{bmatrix} = G_j^{\,LPFG} \begin{bmatrix} R_{j-1}(\delta) \\ S_{j-1}(\delta) \end{bmatrix} \tag{1}$$

$$G_j^{\,LPFG} = \begin{bmatrix} S_{LPFG1} - i(\delta/\gamma_L)S_{LPFG2} & i(q/\gamma_L)S_{LPFG2} \\ -i(q^*/\gamma_L)S_{LPFG2} & S_{LPFG1} + i(\delta/\gamma_L)S_{LPFG2} \end{bmatrix} \tag{2}$$

Where:

δ = detuning parameter
$\gamma_L \equiv (q^2 + \delta^2)^{1/2}$
$S_{\mathrm{LPFG1}} = \cos(\gamma_L \Delta z)$
$S_{\mathrm{LPFG2}} = \sin(\gamma_L \Delta z)$

$R_M(\delta)$ and $S_M(\delta)$ are the amplitudes of the mode fields traversing through a section j of length Δz, where the coupling coefficient $q(j\Delta z)$ is unique for each section j, and $\rho_j = (-q_j^*/|q_j|)\tanh(|q|\Delta z)$ [4, 5]. When using the DLP algorithm, the LPFG structure is divided into M layers separated by a distance Δz, and the main aim is to obtain the strength of the instantaneous scattering points ρ_M, given a valid pair of transmission $R_M(\delta)$ and cross-coupling $S_M(\delta)$ spectra [4]. The spectral fields, $R_M(\delta)$ and $S_M(\delta)$, are periodic with a period of $\delta_w = \pi/\Delta z$. The detuning parameter for uniform LPFGs is defined as $\delta \equiv (1/2)(\beta_a - \beta_b^{\mu}) - (\pi/\Lambda)$, where β_a is the propagation constant of the core mode, β_b^{μ} is the propagation constant of the μth cladding mode and Λ is the grating period [1]. The resonant wavelength of an LPFG structure is defined as $\lambda_{\mathrm{LPFG}} = \Delta n_{\mathrm{eff}}\Lambda$, where Δn_{eff} denotes the difference between the effective refractive indices of the core and the cladding [1]. By letting all the coupling take place at a single point, i.e. $|q| \to \infty$, while the product $q\Delta z$ remains constant, the distributed coupling process can be separated into two parts that consists of replacing the transfer-matrix matrix G_j^{LPFG} by a product of two transfer matrices, $G_{\Delta}^{\mathrm{LPFG}}$ (pure propagation between instantaneous scattering points in LPFG) and G_{ρ}^{LPFG} (mode-coupling in the jth section) [4].

$$G_{\rho}^{LPFG} = \left(1 + |\rho|^2\right)^{-1/2} \begin{bmatrix} 1 & \rho \\ -\rho^* & 1 \end{bmatrix} \tag{3}$$

$$G_{\Delta}^{LPFG} = \begin{bmatrix} \exp(i\delta\Delta z) & 0 \\ 0 & \exp(-i\delta\Delta z) \end{bmatrix} \tag{4}$$

Where:

$1 \le j \le M$

The discrete coupling ratio in the LPFG is then simply expressed as $\rho_M = s_M(0) / r_M(0)$, where the time-domain coefficients are defined as [4]: $R_j(\delta) = \sum r_j(\tau)\exp(\mathrm{i}2\Delta z\delta\tau)$ and $S_j(\delta) = \sum s_j(\tau)\exp(\mathrm{i}2\Delta z\delta\tau)$, where $\tau = 0,1,\ldots,M$. Since the value of ρ_M is known at the final layer, we can now remove this layer and obtain the impulse responses of layer $M - 1$ as follows [4, 5]:

$$r_{M-1} = \left[r_M(\tau) + \rho_M^* s_M(\tau)\right] / \sqrt{|\rho_M|^2 + 1} \tag{5}$$

$$s_{M-1}(\tau - 1) = \left[s_M(\tau) - \rho_M r_M(\tau)\right] / \sqrt{|\rho_M|^2 + 1} \tag{6}$$

The DLP procedure of reconstructing a LPFG from a complex spectrum profile is summarised in [4, 5, 8].

2.2 Grating synthesis by flip-flop optimisation method

For many years, the flip-flop method has been used extensively for the synthesis of thin-film structures (with practically realisable refractive index profiles) [9, 10]. The flip-flop method was effective in obtaining an equivalent thin-film structure exhibiting either a low or high refractive index at all layers (exhibiting equal thickness). In this paper, results are presented where the flip-flop method was used to synthesise an LPFG originally designed using the DLP method. The results obtained from the flip-flop method are intended to be used for the fabrication of an LPFG in single-mode fibre using a point-by-point fabrication technique [11]. The flip-flop method is described as follows:

1. Divide the LPFG to exhibit equal grating periods. Since the grating was originally designed by using the DLP method, the grating does not need to be divided to exhibit equal grating periods. Take note of the π phase shifts at each zero point of the refractive index profile of the synthesised LPFG;
2. Assign initial refractive index values to each grating period using a suitable starting index profile design;
3. Evaluate a fitness function that represents performance of the starting index profile design;
4. Move through the synthesised LPFG and change the state (i.e. refractive index) of each grating period one-by-one. The fitness function has to be calculated for each flipped state. A grating period can exhibit either a low or high refractive index value. The superior fitness function value for a particular flipped state is retained and used in subsequent calculations;
5. If the fitness function improved after evaluating all grating periods in a single pass, step 4 is repeated, otherwise the synthesis process is complete.

3. NUMERICAL RESULTS

3.1 Design of a broadband LPFG using the DLP method

In this section an LPFG is reconstructed from a complex spectrum profile. The cross-coupled power spectrum has a flat-top, nearly rectangular passband described by a "Super-Gaussian" function [4]:

$$S_M(\delta) = \sqrt{T} \times \exp\left[-\left(\delta / \delta_{pb}\right)^{20}\right] \tag{7}$$

where the maximum cross-coupled power (T) in the passband is –0.46 dB. The passband's full width at half-maximum (δ_{pb}) is 25 nm and the resonant wavelength (λ_{LPFG}) is 1562 nm. The grating chirp is 8.3 nm/cm. The effective refractive index difference (Δn_{eff}) between the guided mode and fifth-order cladding mode is 3.4×10^{-3}. The reference grating period (Λ) equals 459 μm. The grating length (L_{LPFG}) is 30 mm and the number of layers used to reconstruct the LPFG is 34, where $M = L_{\mathrm{LPFG}} / \Delta z$. During the simulation, the number of wavelengths (X) is equal to 1000. The power transmitted by the core mode and cladding mode are shown in Figure 1. The transmission spectrum is kept above –11 dB, exhibits a full-width half maximum (FWHM) bandwidth of 24.9 nm, and has no sidelobes. The ripple variation of the

transmission spectrum and cross-coupled spectrum are 0 dB and 1.2×10^{-3} dB, respectively. Figure 2 shows the coupling coefficient and index modulation of the synthesised LPFG. The LPFG has uniform grating periods and a refractive index profile that exhibits a sinc-like envelope, where there exists a π phase shift at each minimum point [4, 5]. Zhang et al. observed similar results after the DLP method was used to reconstruct an LPFG [5]. An error function is used for the measurement of the difference between the synthesised and desired cross-coupling spectrum of an LPFG. The error function is used to evaluate the performance of the synthesis method and is expressed as: $d\{S_{SYN}, S_{DES}\} = \sum (|S_{SYN,k}| - |S_{DES,k}|)^2$, where $S_{SYN,k}$ and $S_{DES,k}$ are the kth value of the synthesised and desired cross-coupling spectrum, respectively [8]. The temporal performance ($R_ç$) metric is commonly used for comparing the performance of different algorithms for the solution of the same problem [12]. Temporal performance is commonly expressed in solutions per second (sol/s) and attains a maximum when the algorithm's run-time is at a minimum [12]. The reconstruction of the LPFG took 768 milliseconds using MATLAB® on a 2.2 GHz Athlon K7 computer. The DLP algorithm reproduced the original cross-coupling power spectrum with an absolute error of almost 0%. The maximum error in computing the cross-coupled power in the simulation is of the order of 10^{-4} dB. The absolute error is calculated in the wavelength region, 1489 to 1635 nm. The DLP algorithm produced 655.5 KFLOPS within 768 ms of execution time. The temporal performance of the layer-peeling algorithm was calculated at 1.3 sol/s.

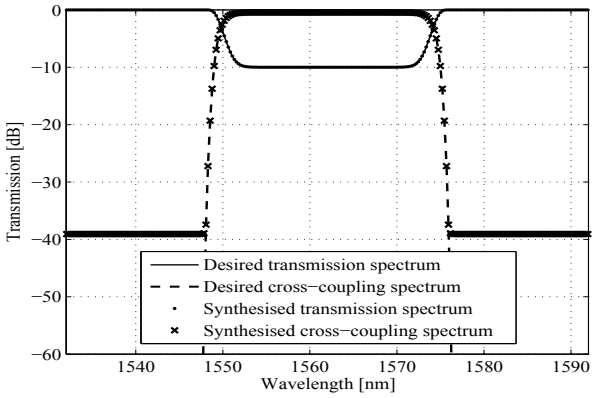

Figure 1: Spectrum results associated with the synthesised LPFG compared to results of desired LPFG

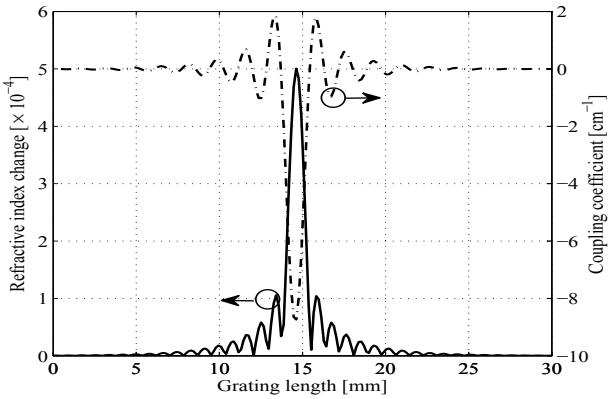

Figure 2: Refractive index modulation and coupling coefficient of synthesised LPFG

In practice the synthesised index modulation profile illustrated in Figure 2 will be difficult to implement due to its complex profile. Most often, it is difficult to develop a fabrication system that delivers the required accuracy [11]. The synthesised refractive index profile illustrated in Figure 2 is segmented using the grating period (i.e. 459 μm) to consider practical fabrication issues. Unfortunately, the LPFG structure, considering practical fabrication issues, differs from the original synthesised LPFG in that the transmission spectrum does not exhibit a perfect flat-top profile and in that the spectrum bandwidth decreases.

3.2 Design of a broadband LPFG using the flip-flop optimisation method

The refractive index change profile (considering fabrication issues) can be simplified even further to ease the LPFG fabrication process by using the flip-flop method. The aim is to retain the grating periods as they are, but to change the index change values to exhibit either a low or high index change at each grating period – essentially a "digital" design using only two refractive index values. Figure 3 illustrates the transmission spectrum obtained for the core mode and cladding mode after implementing the flip-flop method in conjunction with the DLP method. The results were obtained after three iterations of the flip-flop method in less than 80 seconds. In Figure 3, the transmission loss of the flip-flop synthesised LPFG exhibits a transmission loss greater than > 6 dB within the stopband. The index change profile of the flip-flop synthesised LPFG illustrated in Figure 4 will ease the LPFG fabrication process. New positions exist for π phase shifts along an LPFG, when the flip-flop method is implemented. Figure 5 illustrates that the dispersion for the optimised filter is small (4 ps/nm) when the LPFG is reconstructed using the DLP

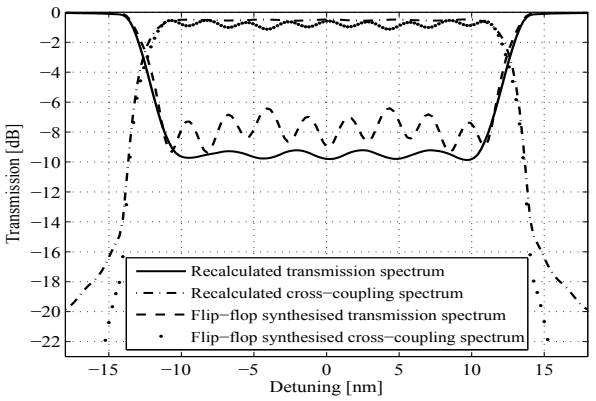

Figure 3: Spectrum results associated with the flip-flop synthesised LPFG compared to spectra of DLP synthesised LPFG with fabrication issues considered

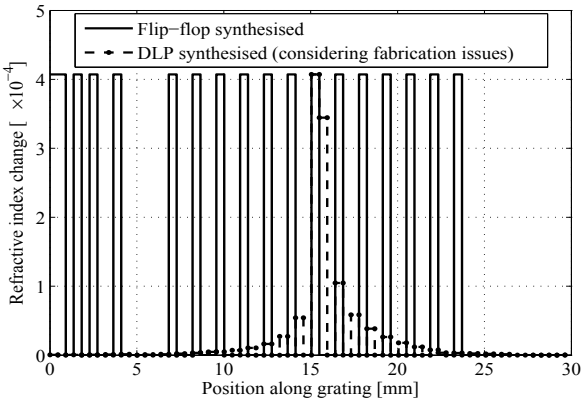

Figure 4: LPFG index modulation profile results obtained using the practical DLP method and flip-flop method

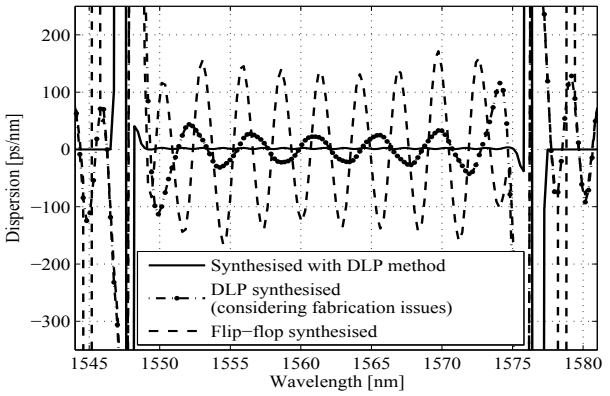

Figure 5: Predicted dispersion of optimised LPFG obtained using the DLP method and flip-flop method

method, but increases when the filter structure results are adjusted for practical implementation, especially when the flip-flop method is used in conjunction with the DLP method. The flip-flop method does not do a good job of reproducing the transmission and cross-coupling spectrum of the LPFG synthesised using the DLP method, resulting in an absolute error of ~4%. The maximum error in computing the transmission power in the flip-flop simulation is of the order of 10^{-1} dB. The flip-flop algorithm produced 72.1 KFLOPS within 78 seconds of execution time. The temporal performance of the flip-flop algorithm was calculated at 1.3×10^{-2} sol/s.

3.3 Discussion

In this paper, LPFGs have been synthesised using the DLP method and flip-flop method. These synthesis methods were used to reconstruct an LPFG structure from a complex spectral profile. The DLP method (discussed in Section 3.1) reconstructed an LPFG efficiently, resulting in an absolute error of almost 0% and a temporal performance of 1.3 sol/s. A high-precision LPFG fabrication system would be required to induce the synthesised refractive index change profile in an optical fibre. The flip-flop method (discussed in Section 3.2) could not reconstruct an LPFG efficiently. The flip-flop method exhibits an absolute error of ~4% and a temporal performance of 1.3×10^{-2} sol/s. The flip-flop method produced a much simpler refractive index change profile compared to the DLP method, but still exhibited π phase shifts at discrete points in the synthesised refractive index change profile. The temporal performance metric was used to compare the performance of different algorithms for the solution of the same problem. It was calculated that the DLP method has the highest performance and executes in the least amount of time.

4. LPFG FABRICATION AND RESULTS

The experimental set-up discussed in [11] was used to fabricate the broadband LPFG. The grating was fabricated in photosensitive single-mode fibre using a TEM_{01*} - mode CO_2 laser (Edinburgh Instruments PL2-M) by implementing the point-by-point fabrication method. Figure 6 illustrates the refractive index change profile of the synthesised LPFG considering practical fabrication issues, as well as the index change profile implemented during the grating fabrication process. The index modulation profile implemented during LPFG fabrication is narrow and exhibit a maximum index change of 3.8×10^{-4} near the centre of the grating. The index change profile implemented during LPFG

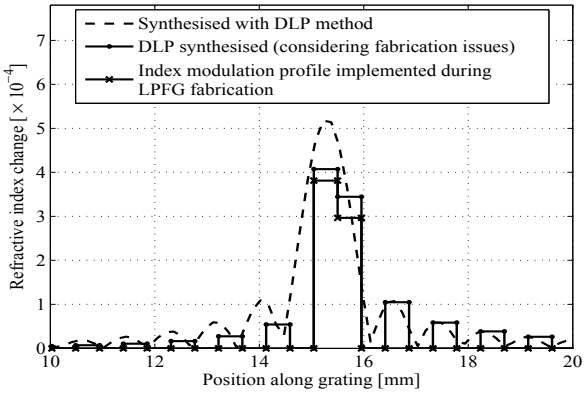

Figure 6: Index change profile implemented during fabrication of complex LPFG designed with DLP method

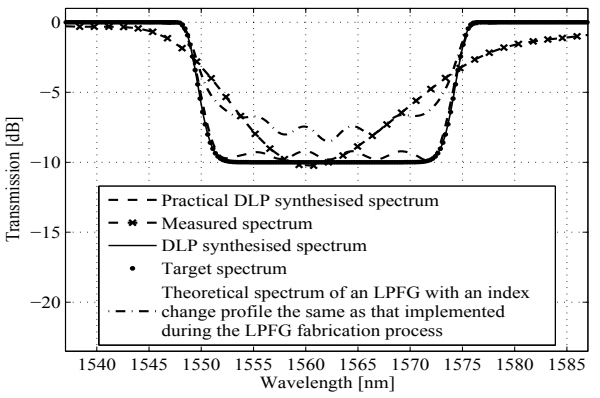

Figure 7: Spectra simulated and measured after fabricating complex LPFG designed with DLP method

fabrication (line-cross graph) can resemble the index change profile considering fabrication issues (line-dot graph) more closely by decreasing shutter exposure time. Figure 7 illustrates the transmission spectrum measured after the complex LPFG was fabricated. The measured spectrum did not exhibit a flat-top, but exhibits minimal sidelobes and a FHWM stopband bandwidth close to the target spectrum (dotted graph). The measured spectrum exhibits a FWHM stopband bandwidth of ~27 nm and a maximum transmission loss of 10.3 dB at ~1561 nm. Figure 7 shows that the measured transmission spectrum (dash-cross graph) differs from the theoretical transmission spectrum (dash-dot graph). The reason for this could be attributed to grating imperfections or accumulation of numerical errors and phase errors when the DLP algorithm is implemented during the simulation of the LPFG transmission spectrum (using index change profile implemented during LPFG fabrication process). The greater the difference between the original DLP synthesised index change profile (dashed graph of Figure 6) and the practical index change profile (line-cross graph of Figure 6), the greater the grating phase error will be. The grating fabrication set-up in [11] does place a limit on the accuracy that can be achieved in manufacturing LPFGs designed with the DLP method. The LPFG experimental results obtained with the DLP algorithm were not good enough, since the LPFG transmission spectrum did not resemble a flat-top type spectral profile. However, the measured spectrum did exhibit a high transmission loss and broad bandwidth in the stopband. The theoretical results obtained from the flip-flop method were not considered in experiments, because the simulation results obtained from the DLP algorithm was used by the flip-flop method to simplify the index change profile. It was expected that if no decent experimental results were obtained with the DLP algorithm, better experimental results would not be obtained with the aid of the flip-flop method either, unless a more accurate LPFG fabrication set-up is used. To our knowledge, this was the first time a point-by-point fabrication method was used to manufacture a DLP synthesised LPFG.

5. APPLICATIONS

5.1 Bragg grating sensor interrogated by an LPFG

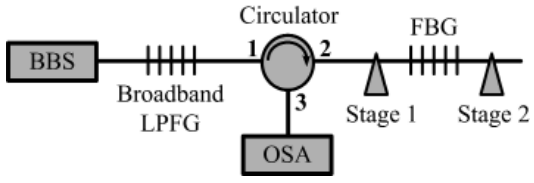

Figure 8: Schematic diagram of FBG sensor system with LPFG as interrogation element

Figure 8 illustrates a system that operates on the principle of using a broadband LPFG to interrogate a fibre Bragg grating (FBG) strain sensor, which is based on strain

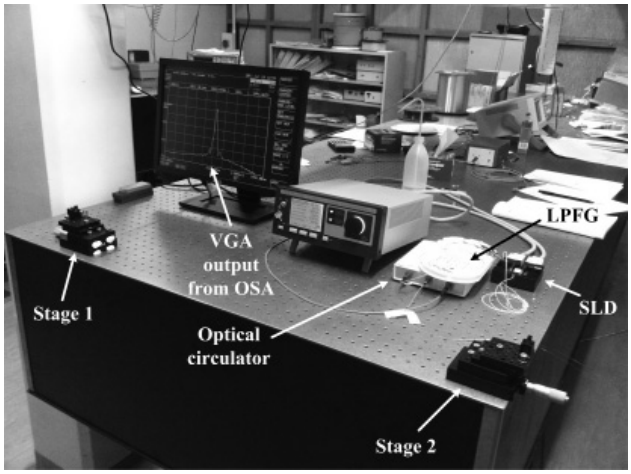

Figure 9: Illustration of the experimental set-up for fibre grating sensor interrogation

related optical intensity measurements. The experimental set-up consisted of a superluminicent-diode (SLD) light source, broadband LPFG, optical circulator, two translation stages, a narrowband FBG and an optical spectrum analyser (Ando AQ6315B). Each translation stage contains one fibre clamp. The distance between the fibre clamps is ~1 m before the fibre is strained. Figure 9 illustrates an image captured of the experimental set-up for fibre grating sensor interrogation. The LPFG length is 40 mm and exhibits a 1567.7 nm resonant wavelength (λ_{LPFG}) when mode-coupling is performed to the fifth-order cladding mode. The broadband LPFG is used as an edge filter that yields an almost linear relationship between the wavelength shift of the FBG and the detected light intensity at different strain-induced values [13]. The FBG length is 5 mm and exhibits a resonant wavelength of 1546.4 nm. A FBG is a reflection filter that reflects light at a specific resonant wavelength [6]. During the experiments the resonant wavelength (λ_{FBG}) of the FBG is located at the negative slope side of the LPFG curve (i.e. intensity-descending side of LPFG transmission band) as shown in Figure 10. The reflected FBG power decrease when λ_{FBG} shifts to longer wavelengths. Figure 11 and 12 illustrates the shift in λ_{FBG} and decrease in light intensity

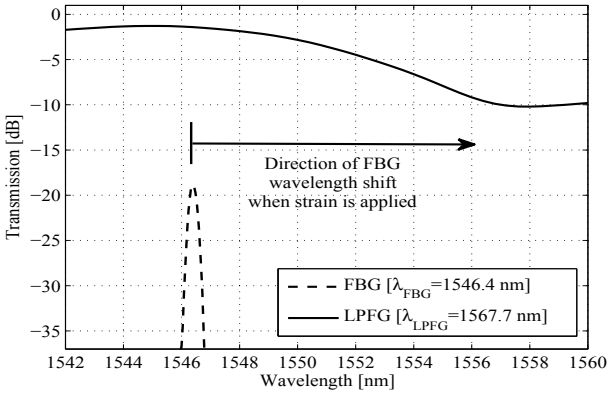

Figure 10: Spectrum of FBG strain sensor and LPFG employed as edge filter

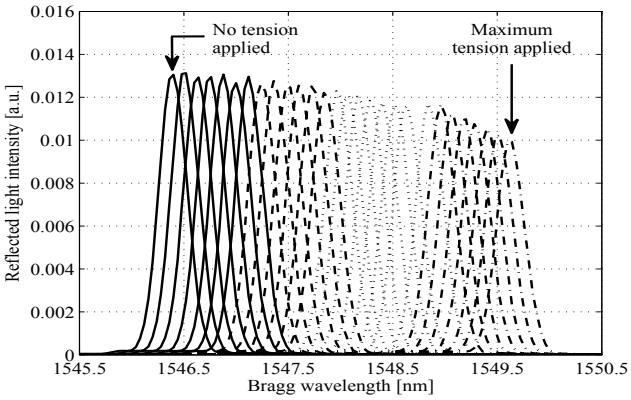

Figure 11: FBG resonant wavelength versus reflected light intensity

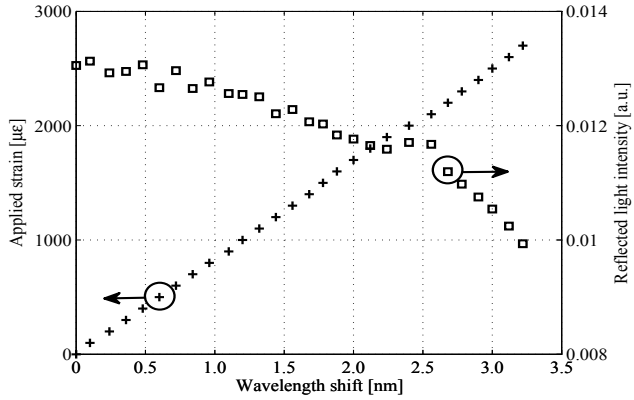

Figure 12: FBG wavelength shift versus applied strain and reflected light intensity

by varying applied strain from 0 to 2700 με. The FBG is strained by moving the second translation stage as shown in Figure 8. The FBG produced satisfactory results when it was placed under tension, resulting in a maximum wavelength shift of 3.2 nm at a translation stage displacement of 2.7 mm. Compared to other experiments where narrowband LPFGs are utilised [13, 14], the broadband LPFG used in this particular experiment exhibits steeper side skirts, which results in the decrease in light intensity to be more rapid when strain is applied to the FBG. Using a LPFG exhibiting steep side skirts in a FBG strain sensing system can be useful in environments where small changes in fibre strain and significant changes in optical light intensity need to be monitored. To our knowledge, this is the first time results are presented where a broadband CO_2-laser-induced LPFG is used to interrogate a FBG strain sensor.

5.2 Wavelength-tuneable OADM using broadband LPFGs and a narrowband FBG

Figure 13 illustrates an OADM utilising a pair of broadband LPFGs and a narrowband FBG, designed for operation in a dense wavelength-division multiplexing (DWDM) network. Evanescent field coupling in an

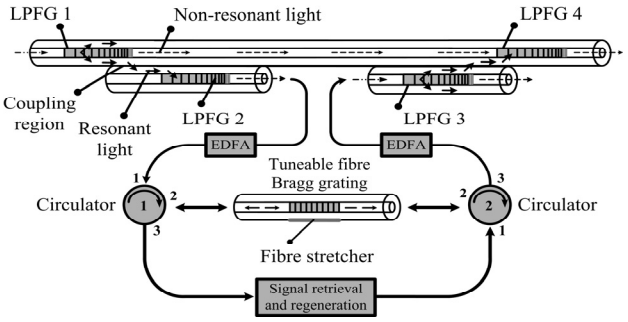

Figure 13: Broadband ADM designed for WDM network

optical fibre-based wavelength-selective coupler (WSC) allow broadband light to be transferred between two fibres containing non-uniform LPFGs [15]. Since the multiplexing part of the OADM illustrated in Figure 13 is the mirror image of the de-multiplexing part, only results obtained for the de-multiplexing part are presented. Figure 14 illustrates the experimental set-up of the de-multiplexing part of the OADM. A wavelength-tuneable laser source (Agilent 81600B) was used to transmit a specific wavelength channel at 1 mW through the WSC. An EDFA was used to restore the power level of the output signal obtained from the WSC to its original level. A tuneable FBG (with 37.2% peak reflectivity) is used to select a specific wavelength channel from the broadband light routed through the WSC. The resonant wavelength of the FBG is 1549.3 nm when no fibre strain is applied. The results shown in Figure 15 were obtained from an optical spectrum analyser (Yokogawa AQ6317C). Figure 13 illustrates that the non-resonant wavelengths travelling beyond the FBG are routed to the multiplexing part of the OADM. All signals exiting the second circulator are pre-amplified before multiplexed on the original fibre link.

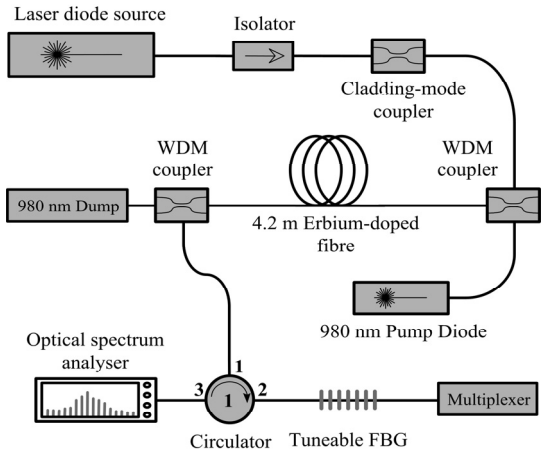

Figure 14: Schematic diagram of experimental set-up for the de-multiplexing part of the OADM

6. CONCLUSION

We have shown that the DLP method can be used successfully to reconstruct broadband LPFGs from a complex spectrum. The DLP method has the highest performance and executes in the least amount of time, but

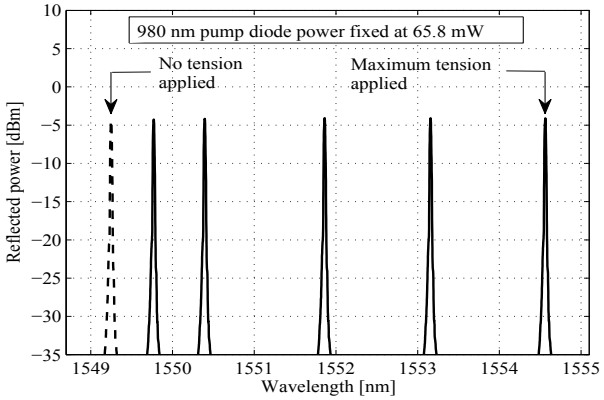

Figure 15: Power spectra of injected wavelength channels

results in index modulation profiles that are difficult to implement in practise. When the flip-flop method is used in conjunction with the DLP method, much simpler LPFG index modulation profiles are obtained, which may be implemented in a LPFG fabrication process. The flip-flop method does not require a complex initial design, and has a rapid convergence. The application of using broadband LPFGs in the field of telecoms and sensing was experimentally demonstrated through the discussion of possible applications. Precise control of the induced index change in the fibre core is of utmost importance in order to manufacture LPFGs that resemble the target spectrum more accurately. The utilisation of the modified DLP and flip-flop synthesis methods in conjunction with an automated fabrication system shows great promise for the manufacture of high-performance LPFGs for application in various industries in the future.

7. ACKNOWLEDGEMENTS

The authors thank CBI Electric (Pty) Ltd, Ericsson SA (Pty) Ltd, Telkom (Pty) Ltd, the National Laser Centre, THRIP, the NRF and the University of Johannesburg for their support as well as Dr. Rodolfo Martinez Manuel for manufacturing the FBGs used in the sensing experiments.

8. REFERENCES

[1] A. M. Vengsarkar, J. R. Pedrazzani, J. B. Judkins, P. J. Lemaire, S. Bergano, and C. R. Davidson: “Long-period fiber grating based gain equalizers”, *Optics Letters*, Vol. 21, No. 5, pp. 336-338, 1996.

[2] Y. G. Han, S. B. Lee, C. S. Kim, and M. Y. Jeong: “Tuneable optical add–drop multiplexer based on long-period fiber gratings for coarse wavelength division multiplexing systems”, *Optics Letters.*, Vol. 31, No. 6, pp. 703–705, 2006.

[3] S. W. James and R. P. Tatam: “Optical fibre long-period grating sensors: characteristics and application”, *Measurement Science and Technology*, Vol. 14, pp. R49-61, 2003.

[4] J. Brenne and J. Skaar: “Design of grating-assisted co-directional couplers with discrete inverse-scattering algorithms”, *Journal of Lightwave Technology.*, Vol. 21, No. 1, pp. 254-263, 2003.

[5] J. Zhang, P. Shum, S. Y. Li, N. Q. Ngo, X. P. Cheng, and J. H. Ng: “Design and fabrication of flat-band long-period grating”, *IEEE Photonics Technology Letters*, Vol. 15, No. 11, pp. 1558–1560, 2003.

[6] T. Erdogan: “Fiber grating spectra”, *Journal of Lightwave Technology.*, Vol. 15, No. 8, pp. 1277-1294, 1997.

[7] G. W. Chern and L. A. Wang: “Design of binary long-period fiber grating filters by the inverse-scattering method with genetic algorithm optimization”, *Journal of the Optical Society of America A*, Vol. 19, No. 4, pp. 772-780, 2002.

[8] R. Kritzinger and J. Meyer: “Design and fabrication of novel broadband long-period fiber gratings using synthesis techniques”, *Journal of Lightwave Technology*, Vol. 29, No. 8, pp. 1077-1084, 2011.

[9] W. H. Southwell, ”Coating design using very high- and low-index layers”, *Applied Optics*, Vol. 24, No. 4, pp. 457-460, 1985.

[10] J. A. Dobrowolski, ”Comparison of the Fourier transform and flip-flop thin-film synthesis methods”, *Applied Optics.*, Vol. 25, No. 12, pp. 1966-1972, 1986.

[11] R. Kritzinger, D. Schmieder and A. Booysen: “Azimuthally symmetric long-period fibre grating fabrication with a TEM_{01} -mode CO_2 laser”, *Measurement Science and Technology.*, Vol. 20, pp. 034004-, 2009.

[12] R. W. Hockney: *The science of computer benchmarking*, SIAM, Philadelphia, chapter 2, 1997.

[13] P. Saidi Reddy, R. L. N. Sai Prasad, K. Srimannarayana, M. Sai Shankar, D. Sen Gupta: “A novel method for high temperature measurements using fiber Bragg grating sensor”, *Optica Applicata.*, Vol. 40, No. 3, pp. 685-692, 2010.

[14] R. W. Fallon, L. Zhang, L. A. Everall, J. A. R. Williams and I. Bennion: “All-fibre optical sensing system: Bragg grating sensor interrogated by a long-period grating”, *Measurement Science and Technology.*, Vol. 9, pp. 1969-1973, 1998.

[15] R. Kritzinger and A. Booysen: "Wavelength-tuneable add/drop multiplexer using broadband transmission filters and a narrowband reflection filter", *Proceedings: SPIE*, Vol. 7004, No. 70042O, 2008.